Macromolecules

pubs.acs.org/Macromolecules Article

Growth and Termination of Cylindrical Micelles via Liquid-Crystallization-Driven Self-Assembly

Liang Gao, Hongbing Gao, Jiaping Lin,* Liquan Wang,* Xiao-Song Wang,* Chunming Yang, and Shaoliang Lin

Cite This: https://dx.doi.org/10.1021/acs.macromol.0c01820 Read Online

ACCESS | Metrics & More | Article Recommendations | Supporting Information

ABSTRACT: Growth and termination of cylindrical micelles with cholesteric liquid crystal (LC) cores (seeds) were achieved experimentally, following the simulation studies of liquid-crystallization-driven self-assembly (LCDSA) of block copolymers. The fluidity of LC cores was proven to be crucial for this success. To a seed solution, the added block copolymer unimers had a high tendency to form new aggregates. The formed aggregates had a less-ordered cholesteric LC structure as compared with those in the seed and subsequently fused with the seeds. After the fusion, the fluidity allowed a rearrangement of the rod blocks within the elongated segments to match the LC structure in the seeds. The fusion and rearrangement were repeated in cycles, which completely consumed the newly formed aggregates and led to a seeded-growth behavior. Under a condition that the interactions between LC blocks are stronger, the newly formed aggregates had smectic LC cores, which fused with the seeds terminating the growth. The termination is attributed to the higher energy barrier for the transition from the smectic LC structure to cholesteric active ends. This work created a theoretical basis for further exploration of living assembly using LC block copolymers, which are building blocks for a wide range of functional materials.

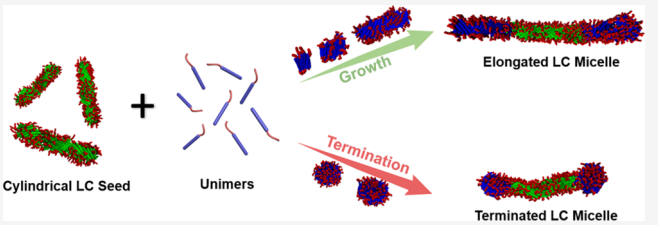

Liquid crystals (LCs) have an orientational or a positional long-range order in at least one direction, while a high degree of mobility of individual molecules retained.[1−3] Crystalline molecules, on the other hand, can crystallize into defined lattices with higher cohesive energy and can undergo epitaxial growth generally.[4−8] It has been reported that crystallization-driven self-assembly (CDSA) of block copolymers in solution gives access to well-defined hierarchical micellar structures based on the epitaxial crystallization.[6−12] This discovery is attracting substantial attention to develop living supramolecular chemistry for precise synthesis of functional supramolecular materials.[13−18] The research on liquid-crystallization-driven self-assembly (LCDSA) of block copolymers has also been inspired,[19,20] but the exact mechanisms remain to be clarified because of the fundamental difference between crystallization and liquid crystallization. The fluidity of LC provides a degree of freedom for the rearrangement of LC structures and accounts for the adaption capability of many LC systems.[1−3,21] We, therefore, examined how the fluidity can be harnessed to circumvent the low epitaxy and achieve control in the growth of LC micelles.

Polypeptide-based rod−coil block copolymers, such as poly(γ-benzyl-L-glutamate)-*block*-poly(ethylene oxide) (PBLG-*b*-PEO) copolymers, undergo micellization in solvents selective for the coil block into various structures with LC structures of PBLG rod blocks as cores.[22,23] PBLG-*g*-PEO graft copolymers assemble into spindle-like aggregates, in which the PBLG rod blocks take a parallel packing along the long axis of micelles (nematic-like LC core), and the ends are partially covered by PEO. By varying the solution conditions, the ends of the micelle can be activated, which induces a hierarchical assembly of micelles or an intramicelle end-to-end cyclization.[24,25] It suggests that interfacial energy is also an important factor, in addition to epitaxy, adjusting the activity for the growth of cylindrical LC micelles. A synergy of this activity and the fluidity of LC structures may circumvent the low epitaxy to realize a control in the growth of LC micelles. We investigated this possibility via theoretical simulations, which effectively guided our experimental exploration.

Brownian dynamics (BD) simulations revealed that the cylindrical micelles with cholesteric LC cores could serve as seeds. When LC block copolymers with a concentration higher than the critical micelle concentration (CMC) were added to the seed solution, only a small fraction of the molecules added to the seeds, while most of them were assembled into new aggregates. Nevertheless, under certain conditions, the newly formed aggregates with cholesteric-like cores fused with the seeds and subsequently underwent rearrangement of the rod

Received: August 4, 2020
Revised: September 20, 2020

blocks in the fluidic core to match the LC structure of the seeds. The repetitions of this fusion and rearrangement consumed the newly formed aggregates, so the system exhibited a seeded-growth behavior. The newly formed aggregates had smectic LC cores when the interaction between the LC block was stronger. These aggregates also fused with the seeds but terminated the growth. The termination was caused by the higher energy barrier for the conversion of the smectic LC core to cholesteric active ends. Herein, we report this theoretical discovery and our experimental investigation guided by this theory.

RESULTS AND DISCUSSION

Self-Assembly of Rod−Coil Block Copolymers in Selective Solvents. A coarse-grained model of R_6C_3 (R, C, and subscripts denote rod block, coil block, and the bead number of each block, respectively) was constructed for the rod−coil block copolymer (Figure 1a). The bead number is

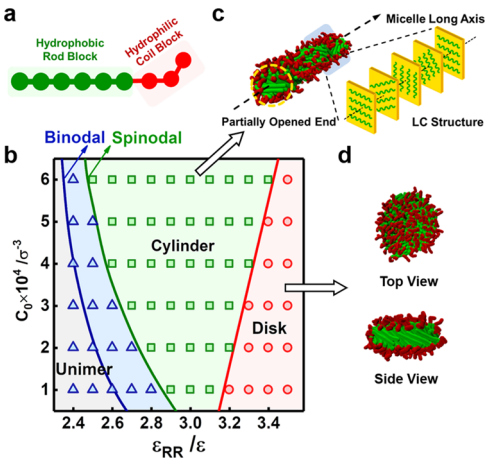

Figure 1. Self-assembly of rod−coil block copolymers. (a) BD model of R_6C_3 for rod−coil block copolymer, R, C, and subscripts denote rod block, coil block, and the bead number of each block, respectively. (b) Morphological diagram for the assemblies of R_6C_3 copolymers in the space of interaction parameter ε_{RR} vs initial copolymer concentration C_0, where σ and ε are the units of length and energy, respectively. (c) Typical cylindrical micelle with partially opened ends and the partially expanded view of the cholesteric LC structure along the long axis of the micelle. (d) Top and side views of the typical disk-like micelle.

chosen based on the molecular structure of the polypeptide-based block copolymers used in our experiments. The amphiphilicity of copolymers was realized by setting different pairwise interaction potentials. The interaction between R blocks (R−R interaction) was modeled with an attractive potential to simulate the hydrophobicity of R blocks, and its strength was described by the interaction parameter ε_{RR}. The C−C and R−C interactions were modeled with repulsive potential, corresponding to the hydrophilic nature of C blocks and the incompatibility between two blocks, respectively.[23,26,27] The assembling behavior was investigated by setting different pairwise interaction parameters (see Section S1.1 of Supporting Information).

R_6C_3 can self-assemble into either cylindrical or disk-like micelles in a selective solvent for C blocks (Figure 1). Figure 1b illustrates the morphological diagram for the assemblies of R_6C_3, where C_0 refers to the ratio of chain number to system volume (other parameters are set as constants). As ε_{RR} increases, C_0 required for the onset of assembly (green line in Figure 1b), corresponding to the CMC decreases. The system with a higher ε_{RR} tends to form disk-like aggregates. Figure 1b displays the spinodal and binodal lines. The spinodal line usually refers to the CMC in phase separation, while the area between the spinodal line and the binodal line indicates the formation of thermodynamically unfavorable micelles.[28] Note that the region between two lines is a metastable region where nucleation and growth can occur simultaneously.

The cylindrical micelles are formed via an interdigitated packing of R blocks (Figure 1c). The orientation of the packing plane gradually rotates along the long axis of the micelle, suggesting that the core for the micelles has a cholesteric LC core (Figure S1a,b).[1−3,22,23,27] The coil blocks cover the cholesteric cores, but the two ends have a certain degree of exposure to the solvent. The disk-like micelles have a smectic LC core, in which the R blocks are vertically aligned with a small deviation from the perpendicular direction to the disk plane (Figures 1d, S1c,d).[1−3]

Growth of Cylindrical Micelles Assembled from Rod−Coil Block Copolymers. The cylindrical micelles formed at $C_0 = 3.0 \times 10^{-4}\sigma^{-3}$ were chosen as seeds, to which a new batch of R_6C_3 rod−coil block copolymers was added. When the concentration of the added copolymers (C_0^{2nd}) is located in the metastable region below the CMC (blue region in Figure 1b), the added copolymers can grow on the ends of seeds in a living growth manner.[27] However, the metastable region is usually so narrow that the living growth of LC seeds via adding unimers one-by-one is difficult to be realized experimentally.[19,20,27] Here, we turn our attention to the green region where the concentration is above the CMC, for example, $C_0^{2nd} = 4.0 \times 10^{-4}\sigma^{-3}$ and $\varepsilon_{RR} = 2.7\varepsilon$. This condition favors the formation of cylindrical micelles via self-aggregation.

The assemblies captured at the simulation time of 1.25×10^4 τ and 2.0×10^5 τ are displayed in Figure 2a,b, respectively. As shown in the figures, the added copolymers initially assemble into small aggregates in addition to the growth of seeds (Figure 2a). The newly formed aggregates also exhibit partially opened ends and subsequently fuse with the seeds (Figure 2b). This fusion is mainly driven by the minimization in interfacial energy. Figure 2c shows a typical micelle resulting from the seeded-growth and the expanded view of the core. As shown in the figure, the cores for the seed segment (green) and the elongated segment (blue) have the same periodic variations in the orientation of the chains (Figure S2), suggesting that the expended core has the same cholesteric LC structure. It is worth noting that the cholesteric LC-like cores for the newly formed aggregates are less ordered, and some aggregates do not have a perfect cholesteric order (Figure S4). It suggests that the rod blocks in the aggregates can rearrange themselves to match the cholesteric LC structure in the cores of seeds upon fusion. This rearrangement is attributed to the fluidity of LC structures.[1−3]

To further examine the growth process, the time-dependent concentrations of the remaining unimers C_{unimer} and the newly formed aggregates C_{agg} resulting from the added block copolymers were calculated (see Section S1.1 of Supporting Information). As shown in Figure 2d, C_{unimer} dramatically decreases initially, while C_{agg} rapidly increases (green region), implying that the unimers are quickly consumed and assembled into new aggregates or added to the seeds. Subsequently, C_{unimer} gradually drops to a constant low value,

https://dx.doi.org/10.1021/acs.macromol.0c01820
Macromolecules XXXX, XXX, XXX−XXX

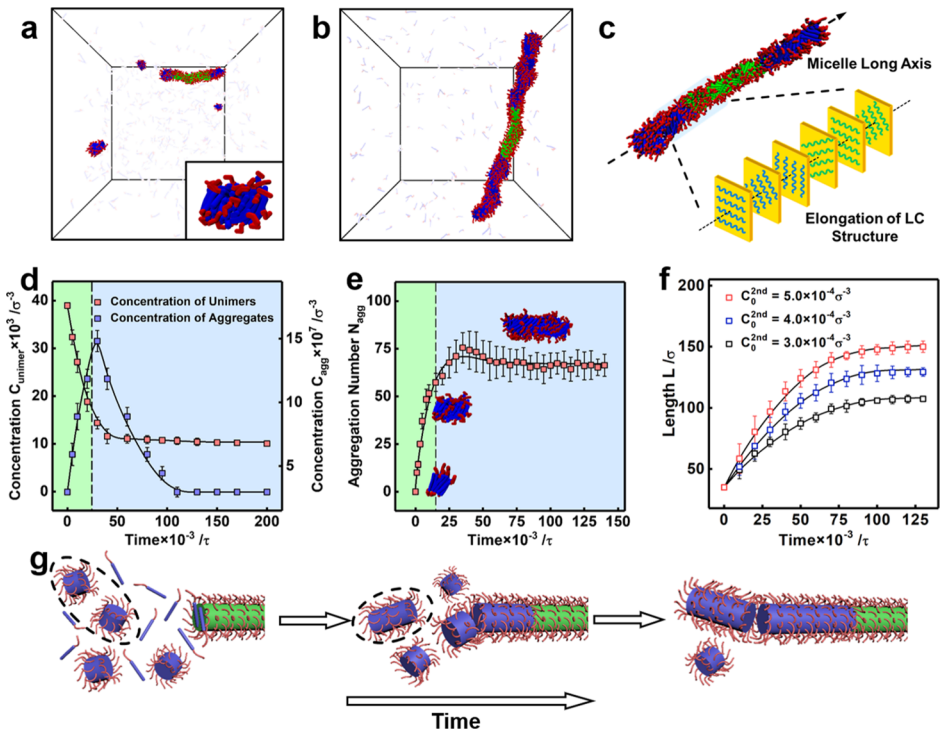

Figure 2. Growth of cylindrical micelles via LCDSA. (a,b) Morphologies of cylindrical micelles at the simulation time of (a) 1.25×10^4 τ and (b) 2.0×10^5 τ, where $C_0 = 3.0 \times 10^{-4}\sigma^{-3}$, $C_0^{2nd} = 4.0 \times 10^{-4}\sigma^{-3}$, $\varepsilon_{RR} = 2.7\varepsilon$, and τ is the unit of time in the simulation, and the free unimers were hyalinized for clarity. (c) Representative micelle after the growth and the partially expanded view of the LC structure along the long axis of the micelle. The rod blocks in the seed and the elongated parts are colored with green and blue, respectively. (d) Temporal variation of the number concentrations of the remained unimers (C_{unimer}) and the formed aggregates (C_{agg}) against the simulation time. (e) Temporal variation of the average aggregation number (N_{agg}) for the formed aggregates, where $C_0 = 3.0 \times 10^{-4}\sigma^{-3}$, $C_0^{2nd} = 7.0 \times 10^{-4}\sigma^{-3}$, and $\varepsilon_{RR} = 2.7\varepsilon$. The green and blue regions in (d,e) denote the aggregation-dominated and fusion-dominated stages, respectively. (f) Temporal variations of the length L for elongated cylindrical micelles at various C_0^{2nd} and the fixed ε_{RR} of 2.7ε. (g) Schematic illustration for the growth process of cylindrical micelles with LC cores.

while C_{agg} decreases in a fast pace and eventually approaches $0\sigma^{-3}$ (blue region). It suggests that the newly formed aggregates tend to be completely consumed via fusion with the seeds.

Figure 2e,f displays the time-dependent average aggregation number (N_{agg}) in the newly formed aggregates and the length of aggregates. As shown in the figures, while the increase in N_{agg} reaches a plateau at a simulation time of 5.0×10^4 τ (Figure 2e), the elongation of the micelles continues (Figure 2f). It supports that the fusion of the newly formed particles can also contribute to the growth of the micelles (the marked region in Figure 2g). Note that these newly formed particles can fuse with each other, and then the fused particles incorporate into the seeds (the marked region in Figure 2g), thereby N_{agg} has a slight decrease at the later stage (Figure 2e). The growth kinetics can be adjusted by C_0^{2nd}. As shown in Figure 2f, the larger C_0^{2nd}, the faster the growth. ε_{RR} is another parameter regulating the kinetic behavior. At the same C_0^{2nd}, the system with a large ε_{RR} ($2.6\varepsilon < \varepsilon_{RR} < 3.0\varepsilon$) has slow growth (Figure S5). The larger ε_{RR} value restricts the mobility of the rod blocks, which lowers the fluidity and slows the kinetics for the rearrangement of the LC core. This result stresses the importance of fluidity of the LC cores in the growth. Therefore, the LCDSA exhibits seeded-growth behavior via cycles of fusion with the seeds and rearrangement of the rod block within the aggregates for the systems with ε_{RR} in the range between 2.6ε and 3.0ε (Figure 2g).

Termination of the Growth. When ε_{RR} is adjusted to a higher level, the added block copolymers form disk-like aggregates with smectic LC cores ($C_0 = 3.0 \times 10^{-4}\sigma^{-3}$, $\varepsilon_{RR} = 3.2\varepsilon$, and $C_0^{2nd} = 3.0 \times 10^{-4}\sigma^{-3}$). As shown in Figure 3a,b, the resulting disk-like aggregates can also fuse with the seeds, but no growth of the cylinder is observed. This deactivation is caused by the low fluidity of the LC core because of large ε_{RR}, which prevents the LC blocks in the disk from rearrangement to match the cholesteric LC structure (see Figure S3). The time-dependent C_{unimer} and C_{agg}, as shown in Figure 3c, indicates that C_{unimer} decreases, and correspondingly C_{agg} increases rapidly (green region) upon the addition of the copolymers. While C_{unimer} continuously drops to $0\sigma^{-3}$ because of a larger ε_{RR} (stronger interaction between the rod blocks), C_{agg} starts to decrease (blue region) because of the fusion of the newly formed disk-like aggregates and their coupling with the seeds (Figure S3). However, a substantial amount of the newly formed aggregates remains and does not add to the seeds, as one can see that C_{agg} eventually levels off at a high level ($2.1 \times 10^{-6}\sigma^{-3}$). This deactivation of the growth can be justified by the conversion of the ends to smectic cores upon the fusion (Figure 1). A higher energy barrier for the structural transition from the smectic core to cholesteric LC ends ceases the growth.

Growth of PBLG-*b*-PNIPAM Micelles. Following the theoretical study, we reviewed our experimental efforts on the assembly of PBLG block copolymers. PBLG with α-helix conformation is the rod block and is possible to form LC structures.[29,30] The strength of intermolecular interactions of PBLG varies with the molecular weight and solvents used for the assembly, which drives the assembly into various

https://dx.doi.org/10.1021/acs.macromol.0c01820
Macromolecules XXXX, XXX, XXX−XXX

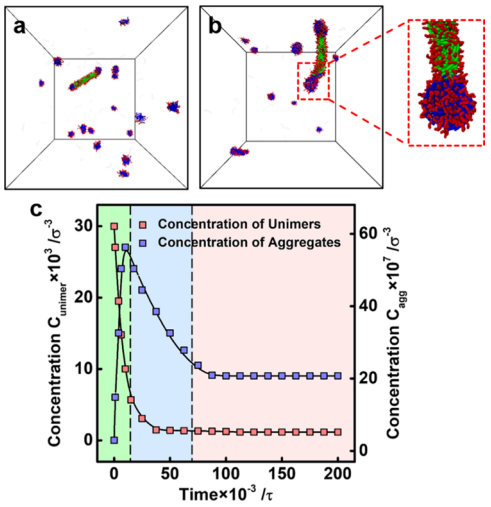

Figure 3. Termination of the growth. (a,b) Morphologies of the aggregates formed at the simulation times of (a) 1.25×10^4 τ and (b) 2.0×10^5 τ, where $C_0 = 3.0 \times 10^{-4}\sigma^{-3}$, $C_0^{2nd} = 3.0 \times 10^{-4}\sigma^{-3}$, and $\varepsilon_{RR} = 3.2\varepsilon$. The partially enlarged view of the marked region is shown in (b). The rod blocks in the seed and the terminated parts are colored with green and blue, respectively. (c) Temporal variation of the number concentrations of the remained unimers (C_{unimer}) and the aggregates (C_{agg}). The green, blue, and red regions are assigned to the aggregation, fusion, and termination stages, respectively.

structures, including spheres, vesicles, or cylindrical micelles.[22,29,30] $PBLG_{178}$-*b*-$PNIPAM_{80}$ (PNIPAM: poly(*N*-isopropyl acrylamide)) block copolymers were used to verify the simulation results, in which PNIPAM is not only water soluble but also thermal responsive for potential material applications. When water was added to the $PBLG_{178}$-*b*-$PNIPAM_{80}$ block copolymer solution (see Figure 4a; the subscript denotes the degree of polymerization for each block), the block copolymers assembled into sphere-like particles (Figure S7a). By using ethanol, less polar than water, as a poor solvent, PBLG-*b*-PNIPAM forms fibers with a polydisperse distribution (Figure S7c). The weaker interaction between the PBLG blocks in the system containing ethanol is responsible for the formation of one-dimensional structures, as we learned from Figure 1. We tried to add a second batch of PBLG-*b*-PNIPAM to the fibers but did not observe an obvious growth behavior. We speculated, based on the simulation, that the solvophobic effect in tetrahydrofuran (THF)/ethanol may be too low to induce the fusion, a crucial step involves in the LCDSA for the growth. To test this idea, methanol was used as a selective solvent for the assembly (Figure S7b). The polarity of methanol lies between that for water and ethanol,[31] so the polymers may assemble into cylindrical aggregates that are capable of fusion.

Seeds were first prepared by adding methanol (2.4 mL), a selective solvent for PNIPAM, to the solution of PBLG-*b*-PNIPAM (8.0×10^{-2} g/L) in THF/dimethylformamide (DMF) mixed solvents (2.0 mL, THF/DMF = 50/1 by volume) (Figure 4b). As indicated by the transmission electron microscopy (TEM) and atomic force microscopy images, cylindrical micelles were formed (Figures 4c, S8). The number average length L_n of the cylinders is ca. 570 nm and the dispersity is low (L_w/L_n = 1.1) (Figure 4c). The methanol content of 54.5 vol % is slightly above the critical content (42.3 vol % in Figure S6), which favors a slow self-aggregation and leads to the low-dispersity of seeds. Both the width and the height of the micelles are ca. 40 nm (Figure S8), which are justified by the cholesteric packing of the PBLG block (ca. 27 nm in length). The structures of the cores were analyzed by the synchrotron radiation wide-angle X-ray scattering (WAXS), which confirms the LC-like micellar cores as predicted by simulations (Figure 4j,k).

A solution of PBLG-*b*-PNIPAM unimers in DMF (2.0 g/L, 25 μL) was added to the seed solution (4.4 mL). The mixed solution containing seeds ($C_0 = 3.6 \times 10^{-2}$ g/L) and the added polymer ($C_0^{2nd} = 1.13 \times 10^{-2}$ g/L) was aged before characterization. Note the C_0^{2nd} is higher than the CMC according to the control experiment without seeds (see Figure S10). Figure 4d–f shows the TEM images for the sample after aging for 6, 12, and 48 h, from which the length of the cylinders is estimated and illustrated in Figure 4g. As shown in Figure 4g, the seeds gradually grow to 1687 nm after aging for 48 h (L_w/L_n = 1.28). Based on this length, it is calculated that all added unimers are aggregated to the seeds and contribute to the growth.

To confirm this seeded-growth behavior, we performed a control experiment by adding a solution of PBLG-*b*-PNIPAM unimers in DMF to methanol/THF mixed solvents. The resulting solution did not contain seeds (C_0 = 0 g/L). As shown in Figure 4h, the solution barely shows growth behavior, while the growth of L_n is obvious for the solutions containing the seeds. The control experiment without the preassembled seeds indicates the self-aggregation of added unimers (for the control experiment details, see Section S2.6 of Supporting Information). Moreover, the growth rate for the solution containing the seeds ($C_0 = 3.6 \times 10^{-2}$ g/L) is dependent on C_0^{2nd}. The higher C_0^{2nd}, the faster the growth rate (Figures 4h, S9), which also supports seeded-growth behavior. The seeded-growth process was followed by dynamic light scattering (DLS) experiments. The resulting DLS profiles for the growth ($C_0 = 3.6 \times 10^{-2}$ g/L and $C_0^{2nd} = 4.54 \times 10^{-3}$ g/L) are illustrated in Figure 4i. As shown in the figure, a small peak with R_h of ca. 25 nm appears upon the addition of the block copolymers and disappears after 30 h. Over this period, R_h for the seeds (110 nm) increases to 245 and 381 nm at 8 and 30 h, respectively (Figure 4i). The disappearance of the aggregates with a smaller R_h formed at the early stage supports that the seeded-growth involves the formation of new aggregates and their fusion with the seeds. Additionally, some small aggregates can fuse with each other before incorporating into the seeds, which could lead to a broader length distribution in Figure 4g.

Figure 4j shows the WAXS pattern of the dried cylindrical micelle seeds. The multiple diffraction rings demonstrate that there are ordered periodic nanostructures in the cylindrical micelles. The two strong diffraction peaks at q = 3.92 and 12.74 nm^{-1} (Figure 4k) correspond to the distances d of $2\pi/3.92$ = 1.60 nm, and $2\pi/12.74$ = 0.50 nm, respectively, for the periodically ordered nanostructures. The former (q = 3.92 nm^{-1} and d = 1.60 nm) is the distance between two parallel packing PBLG blocks packed within the micelle cores.[32,33] The latter (q = 12.74 nm^{-1} and d = 0.50 nm) is attributed to the helical pitch of PBLG blocks with α-helix conformation (the length is 0.54 nm for the standard α-helix conformation).[34] The intensity for the peak at q = 3.92 nm^{-1} is relatively weak for the formed small aggregates suggesting that the packing of the PBLG block is less ordered. After the growth via fusion, the elongated cylindrical micelles show a sharper peak at q = 3.92 nm^{-1} indicating an improvement in the packing order of PBLG

https://dx.doi.org/10.1021/acs.macromol.0c01820
Macromolecules XXXX, XXX, XXX−XXX

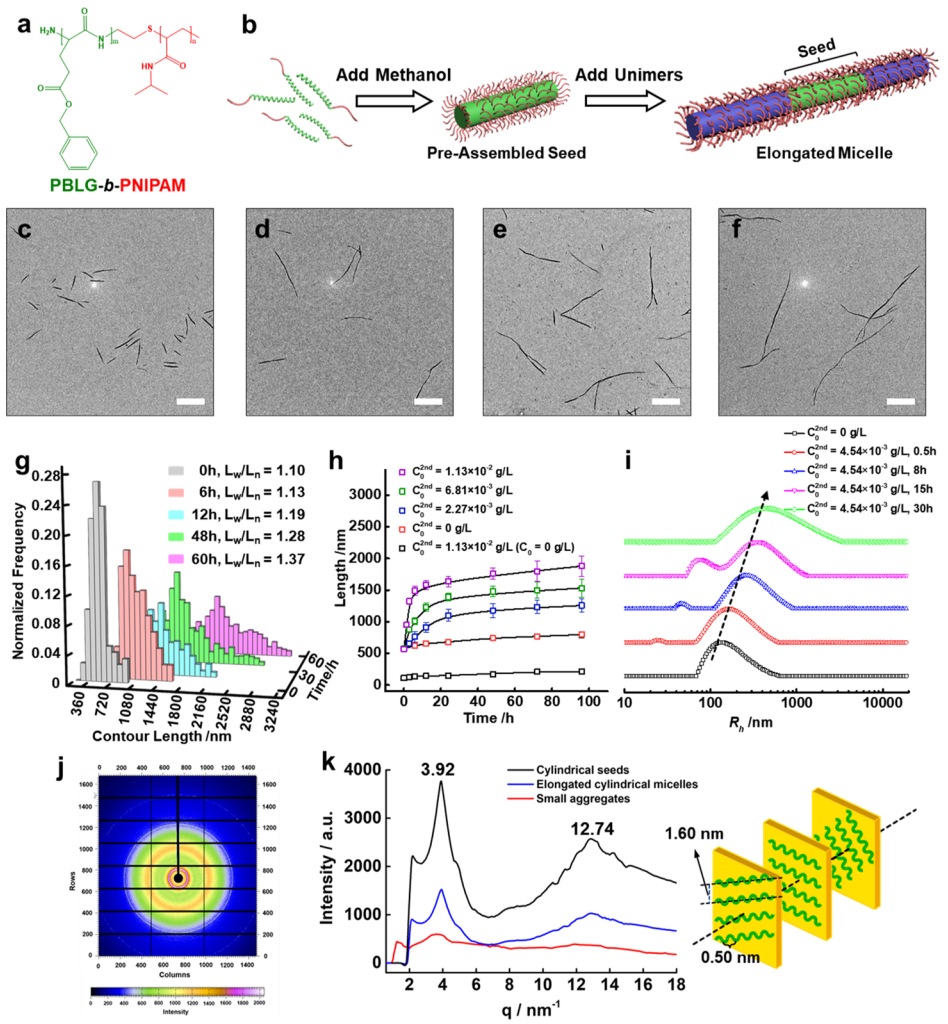

Figure 4. Growth of cylindrical micelles formed by PBLG-*b*-PNIPAM. (a) Chemical structure of the PBLG-*b*-PNIPAM block copolymer. (b) Schematic illustration of the preparation of micelle seeds and the growth of cylindrical seeds. For clarity, cores in the seed and the elongated parts are colored with green and blue, respectively. (c–f) TEM images of the cylindrical seeds and the elongated micelles after adding PBLG-*b*-PNIPAM in DMF to the seed solutions in methanol/THF ($C_0 = 3.6 \times 10^{-2}$ g/L, $C_0^{2nd} = 1.13 \times 10^{-2}$ g/L) for various aging times: (d) 6, (e) 12 and (f) 48 h, respectively. Scale bar: 1 μm. (g) Distribution of the contour length of the elongated cylindrical micelles at various aging times calculated from the TEM experiments. (h) Temporal evolution of the number-average length of cylindrical micelles for the solutions with various C_0^{2nd} at a fixed C_0 of 3.6×10^{-2} g/L, and length evolution of the aggregates in the control experiment ($C_0 = 0$ g/L, $C_0^{2nd} = 1.13 \times 10^{-2}$ g/L). (i) DLS profiles for the solution ($C_0 = 3.6 \times 10^{-2}$ g/L, $C_0^{2nd} = 4.54 \times 10^{-3}$ g/L) at various aging time. The arrow is included to guide the eye. (j) WAXS pattern of the dried micelle seed sample. (k) WAXS spectra of the dried micelle sample (micelle seeds, elongated micelles, and small aggregates).

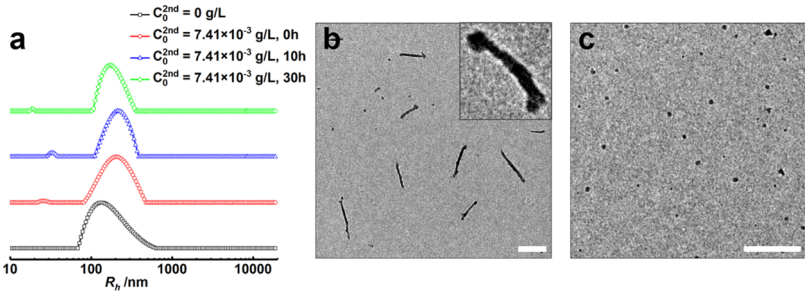

Figure 5. Termination of cylindrical micelles. (a) DLS profiles for the solution of PBLG-*b*-PNIPAM seeds ($C_0 = 3.6 \times 10^{-2}$ g/L and $C_0^{2nd} = 0$ g/L) and those containing both the seeds and added PBLG-*b*-PNIPAM unimers ($C_0 = 3.6 \times 10^{-2}$ g/L and $C_0^{2nd} = 7.41 \times 10^{-3}$ g/L) at various aging times. (b) TEM image for the terminated PBLG-*b*-PNIPAM cylindrical micelles in the system containing water. 1.0 mL water was added to the solution ($C_0 = 3.6 \times 10^{-2}$ g/L and $C_0^{2nd} = 7.41 \times 10^{-3}$ g/L) and the solution was subsequently aged for 10 h. (c) TEM image for the aggregates formed by PBLG-*b*-PNIPAM in the system without seeds. The block copolymers in DMF were added to methanol/THF, then water was added. The ratio for DMF/methanol/THF/water is 1/120/100/50 by volume. Scale bar: 500 nm.

https://dx.doi.org/10.1021/acs.macromol.0c01820
Macromolecules XXXX, XXX, XXX–XXX

blocks. This result verifies the rearrangement of the LC-like structure because of its fluidity as predicted by the simulations.

To terminate the growth, a condition with higher intermolecular interaction of PBLG is required, as guided by our simulations. We first added the unimers in DMF (2.0 g/L, 20 μL) to the solution of seeds (4.4 mL, $C_0 = 3.6 \times 10^{-2}$ g/L). Right after the mixing, water (1.0 mL) was added to the solution to strengthen the interaction between PBLG blocks. The time-dependent R_h of this solution was measured using DLS. As shown in Figure 5a, there is no significant growth of the seeds, suggesting the active ends of the seeds are terminated. TEM experiments were performed for the solution after aging for 10 h. The images shown in Figure 5b contain both the sphere-like particles and cylinders. The average length of the cylindrical aggregates (ca. 680 nm) is close to that for the seeds (ca. 570 nm). The blow-up image (the inset in Figure 5b) indicates that the end of the cylinder is attached to sphere-like aggregates. In a control experiment, PBLG-*b*-PNIPAM block copolymers in DMF (2.0 g/L, 20 μL) were added to methanol/THF/water solvents without the seeds. Sphere-like particles were exclusively formed in this solution (Figure 5c). Therefore, it is confirmed that, with the presence of water, the interactions between the PBLG blocks could be strengthened, leading to the sphere-like aggregates. The fusion of the aggregates with the seeds occurs but terminates the growth. The stronger interaction, assisted by hydrophobic effects, between the rod blocks in the cores of spherical micelles lowers the fluidity, so the rearrangement of LC to match the LC structure of seeds is difficult, and the growth is terminated. This result agrees well with the simulation predictions.

LCDSA Versus CDSA. Unlike CDSA, the epitaxial growth of the LC structure is less possible because of weak cohesive energy.[1−3,19] The synergy of high interfacial energy at the micelle ends, and fluidity of the LC structure, however, compensates the low epitaxy possibly resulting in seeded-growth behavior. The repetitions of the fusion and the rearrangement of the rods in the LC core eventually consume the newly formed aggregates. When ε_{RR} is larger, the added LC block copolymers may self-aggregate into micelles with smectic cores. Upon the fusion, the end is converted to the smectic LC structure, and the energy barrier for the structure-transition prevents the rearrangement of the rod blocks into active cholesteric ends, which terminates the growth. Although the mechanism for the LCDSA seeded-growth is different from CDSA that is mainly based on epitaxy via chain folding (seeded-growth can also occur through a non-chain folding manner in some CDSA systems),[6−9,11,12,18] what we learned from the simulation is also helpful for a better understanding of CDSA. The intermolecular interaction and mobility of the core-forming crystalline chains also appear to be critical factors affecting CDSA as indicated in several reports.[35−37] The interactions between the crystalline block copolymers must be strong enough to induce the assembly.[35] However, the interactions for many crystalline blocks, for example, poly(3-hexylthiophene)-*b*-poly(dimethylsiloxane), are too strong and self-nucleation of added crystalline block copolymers is possible, which prevents the seeds from growth.[36] The presence of a small percentage of common solvent or the use of slightly elevated temperature is necessary to enhance the epitaxial growth.[35−38] By adjusting the intermolecular interactions of the core-forming block via incorporation of a water-insoluble glass segment, CDSA of poly(ε-caprolactone) block copolymers for a defined synthesis in water has been achieved.[39] The results gained in the present work indicated that the fluidity of LC differs the LCDSA behavior with CDSA and can be harnessed for the construction of complex hierarchical nanostructures of LC in a controllable manner.

CONCLUSIONS

In summary, the simulation and experimental work revealed that the LCDSA of LC block copolymers can be regulated for either seeded-growth or growth-termination via adjusting the interaction strength between the LC blocks. The cylindrical micelles with cholesteric cores, assembled from the block copolymers with relatively weaker interaction of LC blocks, acted as seeds. The added block copolymers tended to form new aggregates in addition to adding on the seeds. When the newly formed aggregates have cholesteric LC-like cores, the solution exhibited a seeded-growth behavior. The fusion of the newly formed aggregates with seeds, followed by a rearrangement of the rods in the LC core, accounts for the growth activity of the ends. The added block copolymers assembled into aggregates with smectic LC cores when the interactions between the LC blocks are stronger. The fusion of these aggregates with the seeds converted the end to smectic LC, which terminated the growth because of a large barrier for the structure transition of the ends to the active cholesteric core. This report advanced our understanding of LCDSA and will guide further studies toward a theoretical framework for living/controlled self-assembly of block copolymers.

ASSOCIATED CONTENT

Supporting Information

The Supporting Information is available free of charge at https://pubs.acs.org/doi/10.1021/acs.macromol.0c01820.

Simulation method; rearrangement of LC blocks; polymer synthesis; preparation of aggregates; growth kinetics of cylindrical micelles; and control experiments for the self-aggregation of unimers (PDF)

AUTHOR INFORMATION

Corresponding Authors

Jiaping Lin − *Shanghai Key Laboratory of Advanced Polymeric Materials, Key Laboratory for Ultrafine Materials of Ministry of Education, School of Materials Science and Engineering, East China University of Science and Technology, Shanghai 200237, China;* orcid.org/0000-0001-9633-4483; Email: jlin@ecust.edu.cn

Liquan Wang − *Shanghai Key Laboratory of Advanced Polymeric Materials, Key Laboratory for Ultrafine Materials of Ministry of Education, School of Materials Science and Engineering, East China University of Science and Technology, Shanghai 200237, China;* orcid.org/0000-0002-5141-8584; Email: lq_wang@ecust.edu.cn

Xiao-Song Wang − *Department of Chemistry, Waterloo Institute for Nanotechnology, University of Waterloo, Waterloo N2L 3G1, Canada;* orcid.org/0000-0002-6415-4768; Email: xiaosong.wang@uwaterloo.ca

Authors

Liang Gao − *Shanghai Key Laboratory of Advanced Polymeric Materials, Key Laboratory for Ultrafine Materials of Ministry of Education, School of Materials Science and Engineering, East*

https://dx.doi.org/10.1021/acs.macromol.0c01820
Macromolecules XXXX, XXX, XXX−XXX

China University of Science and Technology, Shanghai 200237, China

Hongbing Gao − *Shanghai Key Laboratory of Advanced Polymeric Materials, Key Laboratory for Ultrafine Materials of Ministry of Education, School of Materials Science and Engineering, East China University of Science and Technology, Shanghai 200237, China*

Chunming Yang − *Shanghai Synchrotron Radiation Facility, Shanghai Institute of Applied Physics, Chinese Academy of Sciences, Shanghai 201204, China;* orcid.org/0000-0001-8008-3675

Shaoliang Lin − *Shanghai Key Laboratory of Advanced Polymeric Materials, Key Laboratory for Ultrafine Materials of Ministry of Education, School of Materials Science and Engineering, East China University of Science and Technology, Shanghai 200237, China;* orcid.org/0000-0003-3374-9934

Complete contact information is available at: https://pubs.acs.org/10.1021/acs.macromol.0c01820

Author Contributions

L.G. and H.G. contributed equally to this work. L.G. performed the simulations and wrote the manuscript. H.G. carried out the experiments. J.L., X.-S.W., and L.W. devised the project and improved the manuscript. All the authors discussed the results and commented on the manuscript.

Funding

This work was supported by the National Natural Science Foundation of China (51833003, 51621002, 21774032, and 21975073), the Project of Shanghai Municipality (16520721900), and Shanghai Sailing Program (20YF1410700).

Notes

The authors declare no competing financial interest.

REFERENCES

(1) Tschierske, C. Development of Structural Complexity by Liquid-Crystal Self-Assembly. *Angew. Chem., Int. Ed.* **2013**, *52*, 8828−8878.
(2) Donald, A. M.; Windle, A. H.; Hanna, S. *Liquid Crystalline Polymers*, 2nd ed.; Cambridge University Press: Cambridge, 2006.
(3) Ciferri, A. Supramolecular Liquid Crystallinity as A Mechanism of Supramolecular Polymerization. *Liq. Cryst.* **1999**, *26*, 489−494.
(4) Flory, P. J. Thermodynamics of Crystallization in High Polymers. IV. A Theory of Crystalline States and Fusion in Polymers, Copolymers, and Their Mixtures with Diluents. *J. Chem. Phys.* **1949**, *17*, 223−240.
(5) Billmeyer, F. W. Lattice Energy of Crystalline Polyethylene. *J. Appl. Phys.* **1957**, *28*, 1114−1118.
(6) Wang, X.; Guerin, G.; Wang, H.; Wang, Y.; Manners, I.; Winnik, M. A. Cylindrical Block Copolymer Micelles and Co-Micelles of Controlled Length and Architecture. *Science* **2007**, *317*, 644−647.
(7) Qiu, H.; Hudson, Z. M.; Winnik, M. A.; Manners, I. Multidimensional Hierarchical Self-Assembly of Amphiphilic Cylindrical Block Comicelles. *Science* **2015**, *347*, 1329−1332.
(8) Qiu, H.; Gao, Y.; Boott, C. E.; Gould, O. E. C.; Harniman, R. L.; Miles, M. J.; Webb, S. E. D.; Winnik, M. A.; Manners, I. Uniform Patchy and Hollow Rectangular Platelet Micelles from Crystallizable Polymer Blends. *Science* **2016**, *352*, 697−701.
(9) He, W.-N.; Xu, J.-T. Crystallization Assisted Self-Assembly of Semicrystalline Block Copolymers. *Prog. Polym. Sci.* **2012**, *37*, 1350−1400.
(10) Kim, Y.-J.; Cho, C.-H.; Paek, K.; Jo, M.; Park, M.-k.; Lee, N.-E.; Kim, Y.-j.; Kim, B. J.; Lee, E. Precise Control of Quantum Dot Location within the P3HT-*b*-P2VP/QD Nanowires Formed by Crystallization-Driven 1D Growth of Hybrid Dimeric Seeds. *J. Am. Chem. Soc.* **2014**, *136*, 2767−2774.
(11) Inam, M.; Cambridge, G.; Pitto-Barry, A.; Laker, Z. P. L.; Wilson, N. R.; Mathers, R. T.; Dove, A. P.; O'Reilly, R. K. 1D vs. 2D Shape Selectivity in the Crystallization-Driven Self-Assembly of Polylactide Block Copolymers. *Chem. Sci.* **2017**, *8*, 4223−4230.
(12) Sun, L.; Pitto-Barry, A.; Kirby, N.; Schiller, T. L.; Sanchez, A. M.; Dyson, M. A.; Sloan, J.; Wilson, N. R.; O'Reilly, R. K.; Dove, A. P. Structural Reorganization of Cylindrical Nanoparticles Triggered by Polylactide Stereocomplexation. *Nat. Commun.* **2014**, *5*, 5746.
(13) Mukhopadhyay, R. D.; Ajayaghosh, A. Living Supramolecular Polymerization. *Science* **2015**, *349*, 241−242.
(14) Kang, J.; Miyajima, D.; Mori, T.; Inoue, Y.; Itoh, Y.; Aida, T. A Rational Strategy for the Realization of Chain-Growth Supramolecular Polymerization. *Science* **2015**, *347*, 646−651.
(15) Ma, X.; Zhang, Y.; Zhang, Y.; Liu, Y.; Che, Y.; Zhao, J. Fabrication of Chiral-Selective Nanotubular Heterojunctions through Living Supramolecular Polymerization. *Angew. Chem., Int. Ed.* **2016**, *55*, 9539−9543.
(16) Zhang, K.; Yeung, M. C.-L.; Leung, S. Y.-L.; Yam, V. W.-W. Living Supramolecular Polymerization Achieved by Collaborative Assembly of Platinum(II) Complexes and Block Copolymers. *Proc. Natl. Acad. Sci. U.S.A.* **2017**, *114*, 11844−11849.
(17) Tritschler, U.; Pearce, S.; Gwyther, J.; Whittell, G. R.; Manners, I. 50th Anniversary Perspective: Functional Nanoparticles from the Solution Self-Assembly of Block Copolymers. *Macromolecules* **2017**, *50*, 3439−3463.
(18) Li, X.; Wolanin, P. J.; MacFarlane, L. R.; Harniman, R. L.; Qian, J.; Gould, O. E. C.; Dane, T. G.; Rudin, J.; Cryan, M. J.; Schmaltz, T.; et al. Uniform Electroactive Fibre-Like Micelle Nanowires for Organic Electronics. *Nat. Commun.* **2017**, *8*, 15909.
(19) Li, X.; Jin, B.; Gao, Y.; Hayward, D. W.; Winnik, M. A.; Luo, Y.; Manners, I. Monodisperse Cylindrical Micelles of Controlled Length with A Liquid-Crystalline Perfluorinated Core by 1D "Self-Seeding". *Angew. Chem., Int. Ed.* **2016**, *55*, 11392−11396.
(20) Jin, B.; Sano, K.; Aya, S.; Ishida, Y.; Gianneschi, N.; Luo, Y.; Li, X. One-Pot Universal Initiation-Growth Methods from A Liquid Crystalline Block Copolymer. *Nat. Commun.* **2019**, *10*, 2397.
(21) Wang, L.; Li, Q. Stimuli-Directing Self-Organized 3D Liquid-Crystalline Nanostructures: from Materials Design to Photonic Applications. *Adv. Funct. Mater.* **2016**, *26*, 10−28.
(22) Ding, W.; Lin, S.; Lin, J.; Zhang, L. Effect of Chain Conformational Change on Micelle Structures: Experimental Studies and Molecular Dynamics Simulations. *J. Phys. Chem. B* **2008**, *112*, 776−783.
(23) Lin, S.; Numasawa, N.; Nose, T.; Lin, J. Brownian Molecular Dynamics Simulation on Self-Assembly Behavior of Rod-Coil Diblock Copolymers. *Macromolecules* **2007**, *40*, 1684−1692.
(24) Zhuang, Z.; Jiang, T.; Lin, J.; Gao, L.; Yang, C.; Wang, L.; Cai, C. Hierarchical Nanowires Synthesized by Supramolecular Stepwise Polymerization. *Angew. Chem., Int. Ed.* **2016**, *55*, 12522−12527.
(25) Yang, C.; Gao, L.; Lin, J.; Wang, L.; Cai, C.; Wei, Y.; Li, Z. Toroid Formation through A Supramolecular "Cyclization Reaction" of Rodlike Micelles. *Angew. Chem., Int. Ed.* **2017**, *56*, 5546−5550.
(26) Grest, G. S.; Kremer, K. Molecular Dynamics Simulation for Polymers in the Presence of A Heat Bath. *Phys. Rev. A* **1986**, *33*, 3628−3631.
(27) Gao, L.; Lin, J.; Zhang, L.; Wang, L. Living Supramolecular Polymerization of Rod-Coil Block Copolymers: Kinetics, Origin of Uniformity, and Its Implication. *Nano Lett.* **2019**, *19*, 2032−2036.
(28) Dayantis, J. Scaling Concepts and the Spinodal and Binodal Curves in Polymer Solutions. *Macromolecules* **1982**, *15*, 1107−1110.
(29) Cai, C.; Lin, J.; Lu, Y.; Zhang, Q.; Wang, L. Polypeptide Self-Assemblies: Nanostructures and Bioapplications. *Chem. Soc. Rev.* **2016**, *45*, 5985−6012.
(30) Cai, C.; Lin, J.; Zhuang, Z.; Zhu, W. Ordering of Polypeptides in Liquid Crystals, Gels and Micelles. *Adv. Polym. Sci.* **2013**, *259*, 159−199.

(31) Hansen, C. H. *Hansen Solubility Parameters: A User's Handbook*, 1st ed.; CRC Press LLC, 2000.
(32) Schmidt, A.; Lehmann, S.; Georgelin, M.; Katana, G.; Mathauer, K.; Kremer, F.; Schmidt-Rohr, K.; Boeffel, C.; Wegner, G.; Knoll, W. Molecular dynamics of "hairy rod" molecules in the solid state: poly(γ-methyl-L-glutamate)-co-(γ-n-octadecyl-L-glutamate) in solution-cast films. *Macromolecules* **1995**, *28*, 5487−5497.
(33) Wang, L.; Huang, Y. Structural characteristics and defects in ethyl-cyanoethyl cellulose/acrylic acid cholesteric liquid crystalline system. *Macromolecules* **2004**, *37*, 303−309.
(34) Tang, H.; Lee, C.-U.; Zhang, D. Thermoreversible gelation of helical polypeptide/single-walled carbon nanotubes and their solid-state structures. *J. Polym. Sci., Part A: Polym. Chem.* **2011**, *49*, 3228−3238.
(35) Shin, S.; Menk, F.; Kim, Y.; Lim, J.; Char, K.; Zentel, R.; Choi, T.-L. Living Light-Induced Crystallization-Driven Self-Assembly for Rapid Preparation of Semiconducting Nanofibers. *J. Am. Chem. Soc.* **2018**, *140*, 6088−6094.
(36) Patra, S. K.; Ahmed, R.; Whittell, G. R.; Lunn, D. J.; Dunphy, E. L.; Winnik, M. A.; Manners, I. Cylindrical Micelles of Controlled Length with a π-Conjugated Polythiophene Core via Crystallization-Driven Self-Assembly. *J. Am. Chem. Soc.* **2011**, *133*, 8842−8845.
(37) Tao, D.; Feng, C.; Cui, Y.; Yang, X.; Manners, I.; Winnik, M. A.; Huang, X. Monodisperse Fiber-Like Micelles of Controlled Length and Composition with An Oligo(p-Phenylenevinylene) Core via "Living" Crystallization-Driven Self-Assembly. *J. Am. Chem. Soc.* **2017**, *139*, 7136−7139.
(38) Tritschler, U.; Gwyther, J.; Harniman, R. L.; Whittell, G. R.; Winnik, M. A.; Manners, I. Toward Uniform Nanofibers with A π-Conjugated Core: Optimizing the "Living" Crystallization-Driven Self-Assembly of Diblock Copolymers with A Poly(3-octylthiophene) Core-Forming Block. *Macromolecules* **2018**, *51*, 5101−5113.
(39) Arno, M. C.; Inam, M.; Coe, Z.; Cambridge, G.; Macdougall, L. J.; Keogh, R.; Dove, A. P.; O'Reilly, R. K. Precision Epitaxy for Aqueous 1D and 2D Poly(ε-caprolactone) Assemblies. *J. Am. Chem. Soc.* **2017**, *139*, 16980−16985.

https://dx.doi.org/10.1021/acs.macromol.0c01820
Macromolecules XXXX, XXX, XXX−XXX